Exchange Reactions of Acetate Ligands and Electrophilic Rhodium–Carbon Bond Activation in Orthometallated Rhodium(II) Compounds with Trifluoroacetic Acid. Crystal Structure of $[Rh_2(O_2CCF_3)_3\{(C_6H_4)PPh_2\}]\cdot2CF_3CO_2H$†

Santiago García-Granda,[*,a] **Pascual Lahuerta,**[*,b] **Julio Latorre,**[b] **Manuel Martinez,**[*,c]
Eduardo Peris,[b] **Mercedes Sanaú**[b] **and M. Angeles Ubeda**[b]
[a] *Departamento de Química Física y Analítica, Universidad de Oviedo, C/Julián Clavería s/n, E-33006-Oviedo, Spain*
[b] *Department de Química Inorgánica, Universitat de Valencia, C/Dr, Moliner 50, E-46100-Burjassot-Valencia, Spain*
[c] *Departament de Quimica Inorgánica, Divisió de Ciencias Experimentals i Matemátiques, Diagonal 647, E-08028 Barcelona, Spain*

Stepwise exchange reactions of acetate groups by trifluoroacetate groups have been observed for $[Rh_2(O_2CMe)_3\{(C_6H_4)PPh_2\}]\cdot2MeCO_2H$ **1**, in $CDCl_3$–CF_3CO_2H at room temperature. The first reaction involves a fast exchange of the two axial molecules of acetic acid as well as the acetate group *trans* to the metallated phosphine. In a second step the exchange of one acetate group *cis* to the metallated phosphine occurs. The exchange of the second *cis* acetate group yielding $[Rh_2(O_2CCF_3)_3\{(C_6H_4)PPh_2\}]\cdot2CF_3CO_2H$ **3**, has been studied by ^1H NMR spectroscopy. This exchange follows a rate equation which is dependent on the concentration of trifluoroacetic acid used, $k_{obs} = (k_1 + k_2[CF_3CO_2H]^{\frac{1}{2}}[Rh_2]$. The partially deuteriated compound $[Rh_2(O_2CCF_3)_3\{(C_6D_4)P(C_6D_5)_2\}]\cdot2CF_3CO_2H$ **3D** in the presence of trifluoroacetic acid undergoes D–H exchange at the *ortho* positions of the phenyl rings of the phosphine. This exchange has been studied at 318 K. The observed D–H exchange is explained by an electrophilic attack at the rhodium–carbon bond by the trifluoroacetic acid, which produces protonation of the *ortho* aromatic carbon atom, and subsequent demetallation followed by a reverse metallation reaction. An X-ray crystal structure determination of compound **3** has been carried out: space group $P2_1/n$ (monoclinic), $a = 12.369(2)$, $b = 21.711(6)$, $c = 13.367(2)$, $\beta = 90.11(2)°$, $Z = 4$ and $R = 0.044$. It contains three trifluoroacetate groups bridging a Rh_2^{4+} unit which has a Rh–Rh bond distance of 2.438(1) Å; the fourth bridging ligand is a triphenylphosphine metallated at one of the *ortho* positions. Two molecules of trifluoroacetic acid occupy the axial positions.

In the course of our investigation on the synthesis and reactivity of orthometallated dirhodium(II) compounds, we have reported the exchange reactions of the bridging acetate groups by CD_3CO_2D in the monometallated compound $[Rh_2(O_2CMe)_3\{(C_6H_4)PPh_2\}]\cdot2MeCO_2H$ **1**.[1] The acetate groups *trans* to the metallated phosphine and the two axial molecules of acetic acid exchange very rapidly in $CDCl_3$–CD_3CO_2D. The kinetic data for the exchange of the other two acetate groups, which is considerably slower, follow a two-term rate equation $k_{obs} = \{k_1 + k_2[CD_3CO_2D]^{\frac{1}{2}}\}[Rh_2]$. Electrophilic attack at one oxygen atom of the bridging acetate groups by a proton of the acetic acid is proposed to be the first and rate-determining step of the exchange process.[1]

Using the isotopically labelled derivative of compound **1** $[Rh_2(O_2CMe)_3\{(C_6D_4)P(C_6D_5)_2\}]\cdot2MeCO_2H$ **1D**, we observed that 90% D–H exchange occurs at the *ortho* positions of the phenyl ring of the phosphine after 3 h in refluxing acetic acid.[1] This observation was explained by consecutive reversible Rh–C bond cleavage and C–H activation processes.

As an example of Rh–C activation, Morrison and Tocher[2] reported that $[Rh_2(O_2CMe)_2\{(C_6H_4)PPh_2\}_2]\cdot2MeCO_2H$ **2** and RCOSH (R = Me, Ph or CMe_3) react under refluxing conditions yielding $[Rh_2(OSCR)_4(PPh_3)_2]$ as the only isolable compound.

The only kinetic study of the exchange of acetate groups with carboxylic acid in this type of compounds has been reported for the reaction of $[Rh_2(O_2CMe)_4]$ with trifluoroacetic acid.[3]

We wanted to explore the reactivity of compounds **1** and **2** with other carboxylic acids under mild reaction conditions as an alternative route to the preparation of other metallated compounds of general composition $[Rh_2(O_2CR)_{4-x}\{(C_6H_4)PPh_2\}_x]\cdot2RCO_2H$ ($x = 1$ or 2). This type of exchange reaction has been extensively used in the preparation of different $[M_2(O_2CR)_4]$ compounds (M = Rh, Mo or W; R = alkyl or aryl).[4]

In this paper we describe the reaction of **1** with CF_3CO_2H at room temperature to yield $[Rh_2(O_2CCF_3)_3\{(C_6H_4)PPh_2\}]\cdot2CF_3CO_2H$ **3**. This is a stepwise reaction which involves some partially substituted compounds. Some rate constants of the last and slowest step of the exchange have been obtained. The crystal structure of compound **3** is also described.

The D–H exchange process has been also studied for **3D**, the isotopically labelled derivative of **3**, in $CDCl_3$–CF_3CO_2H mixtures of variable concentration at 45 °C and some rate constants have been obtained at this temperature.

Results

Exchange of Acetate Groups.—When $[Rh_2(O_2CMe)_3\{(C_6H_4)PPh_2\}]\cdot2MeCO_2H$ **1** is dissolved in a $CDCl_3$–CF_3-

---

† *Supplementary data available:* see Instructions for Authors, *J. Chem. Soc., Dalton Trans.*, 1994, Issue 1, pp. xxiii–xxviii.

CO_2H mixture of variable composition at room temperature, three consecutive processes, of decreasing rate, are detected by ^1H NMR spectroscopy: (*i*) the signal at δ 2.32, due to the *trans* $MeCO_2^-$ group disappears (< 1 min), (*ii*) the signal at δ 1.29, due to the two *cis* $MeCO_2^-$ groups, decreases to half its intensity and shifts slightly (< 5 min) and (*iii*) this signal completely disappears (< 3 h) (Scheme 1). The spectrum of a freshly prepared solution (< 1 min) of **1** in $CDCl_3$–CF_3CO_2H (1:2, 3 cm^3) is consistent with the existence of the partially substituted compound $[Rh_2(O_2CMe)_{2cis}(O_2CCF_3)_{trans}\{(C_6H_4)PPh_2\}]\cdot 2CF_3CO_2H$ **4**, as the main product in solution. This compound has been isolated and characterized by elemental analysis and ^1H and ^{31}P NMR spectroscopy.

When compound **1** is maintained in $CDCl_3$–CF_3CO_2H at room temperature for several hours the totally substituted compound $[Rh_2(O_2CCF_3)_3\{(C_6H_4)PPh_2\}]\cdot 2CF_3CO_2H$ **3**, is formed (Scheme 1). Process (*ii*) is too fast to be monitored by ^1H NMR spectroscopy ($t_{\frac{1}{2}}$ < 300 s). The slowest exchange process (*iii*) has been studied by ^1H NMR spectroscopy, monitoring the disappearance of the signal at δ 1.29 due to the *cis* acetate groups in solutions of **1** in $CDCl_3$–CF_3CO_2H mixtures of variable composition ($[CF_3CO_2H]$ = 0.0–4.63 mol dm^{-3}). The experiments were run at room temperature. In contrast to the behaviour of **1**, the doubly metallated compound $[Rh_2(O_2CMe)_2\{(C_6H_4)PPh_2\}_2]\cdot 2MeCO_2H$ **2** immediately exchanges both bridging acetate groups in the presence of trifluoroacetic acid.

By treating **3** with acetic acid with careful control of the reaction conditions we have isolated the partially exchanged species $[Rh_2(O_2CCF_3)_{2cis}(O_2CMe)_{trans}\{(C_6H_4)PPh_2\}]\cdot 2MeCO_2H$ **5**. Compounds **3**–**5** have been spectroscopically characterized and the crystal structure of compound **3** has been solved.

Exchange Reaction Kinetics.—According to the procedure described in the Experimental section, we obtained k_{obs} values from the slopes of ln R^* *vs*. time. As the modification of the concentration of compound **1** did not show any significant change in the observed rate constants, we assume that this exchange reaction is first order in [**1**]. In order to measure the isotopic effect of the process, we reproduced the experiments by dissolving compound **1** in $CDCl_3$–CF_3CO_2D. For the sake of comparison with acetate exchange studies made with CD_3CO_2D,[1] the same concentrations and temperatures were used. Table 1 shows the observed rate constants for the reactions performed at 298 K at different concentrations of trifluoroacetic acid.

Although the experimental data could be fit to a saturation kinetics rate equation of type $k_{obs} = k_1 + k_2[CF_3CO_2H]/(K + [CF_3CO_2H])$, the above mentioned comparison prompted us to fit these data with rate equation (1),

$$k_{obs} = k_1 + k_2[CF_3CO_2H]^n \qquad (1)$$

with $n = 0.5$ (Fig. 1). No important kinetic isotopic effect is observed for the runs carried out when CF_3CO_2D is used $[k_{2(H)} : k_{2(D)} = 1.14]$. This difference is attributable to changes in the dissociation constant of the acid.

Additional experiments at different temperatures were also run in order to compare the rates of the carboxylate exchange with those obtained for the D–H exchange.

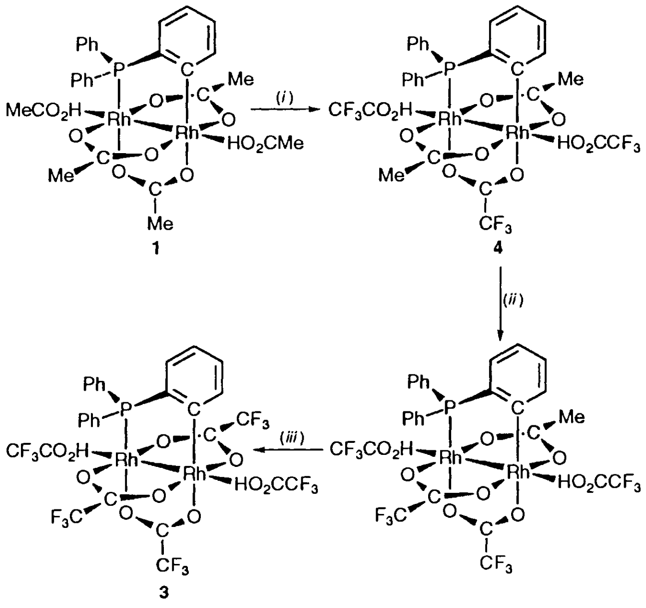

Scheme 1 (*i*) CF_3CO_2H, fast; (*ii*) CF_3CO_2H, $t_{\frac{1}{2}}$ < 300 s; (*iii*) CF_3CO_2H, slow

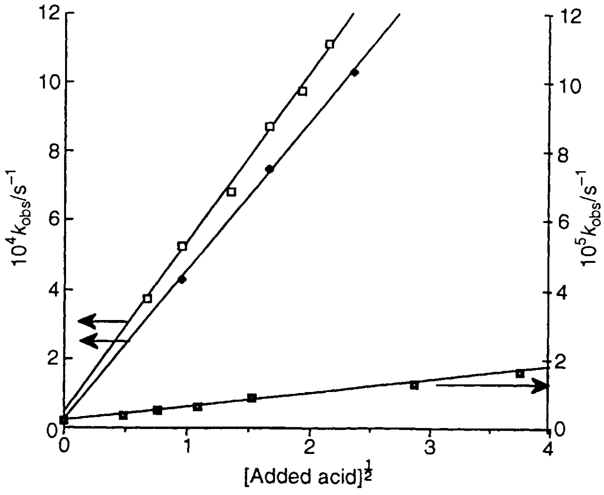

Fig. 1 Plots of the observed rate constants, k_{obs}, *vs*. [added acid]$^{\frac{1}{2}}$ for the reactions studied at 25 °C using CF_3CO_2H (□) and CF_3CO_2D (◆) as compared to those obtained[1] with CD_3CO_2D (■)

Deuterium–Hydrogen Exchange.—When the isotopically labelled compound $[Rh_2(O_2CCF_3)_3\{(C_6D_4)P(C_6D_5)_2\}]\cdot 2CF_3CO_2H$ **3D** reacts with trifluoroacetic acid, we observe two new signals in the ^1H NMR spectrum at δ 6.89 ($^3J_{PH}$ = 10.2 Hz) and 7.49 ($^3J_{PH}$ = 11.1 Hz). These signals, which were already present with very low intensity in the spectrum of **1D** (from which **3D** is obtained) increase in intensity with time. This observation is consistent with a D–H exchange at the *ortho* positions of the phenyl rings of the phosphine yielding a compound of final composition $[Rh_2(O_2CCF_3)_3\{(C_6D_3H)P(C_6D_3H_2)_2\}]\cdot 2CF_3CO_2H$ **3D′**.

Spectroscopically pure samples of **3D** can be easily prepared following the procedure described in the Experimental section. We have measured the rates of the D–H exchange using solutions of **3D** in $CDCl_3$ with different concentrations of CF_3CO_2H at 45 °C. The values of k_{obs} (Table 2) are about two orders of magnitude lower than those obtained for the exchange of acetate bridging groups with trifluoroacetic acid at the same temperature.

Although these values were obtained with much higher uncertainties due to the slow character of the process, the dependence of the observed rate constant with the concentration of acid obeys equation (2).†

$$k_{obs} = k_{Rh\text{-}C}[CF_3CO_2H]^{\frac{1}{2}} \qquad (2)$$

---

* $R = \frac{5}{2}I(MeCO_2^-{}_{cis})/\Sigma I(CH_3)$ where I is the relative integral of the NMR signal.

† This assumption was taken due to its chemical significance, but a saturation kinetics rate law cannot be excluded.

We have monitored the reaction of **3D** in $CDCl_3$ with different concentrations of CF_3CO_2D at 45 °C. We find that the corresponding k_{obs} are four times smaller than for the previous reaction of **3D** with CF_3CO_2H.

No D–H exchange is observed for the isotopically labelled doubly metallated compound $[Rh_2(O_2CMe)_2\{(C_6D_4)P(C_6D_5)_2\}_2]\cdot 2MeCO_2H$, **2D'**, after long reaction times (36 h) at 50 °C.

Discussion

The above described data show that the k_1 and k_2 values are about two orders of magnitude higher than when CD_3CO_2D is used.[1] This behaviour is due to the higher strength of the trifluoroacetic acid. The D–H exchange in **1D** can be explained by an electrophilic attack at the rhodium–carbon bond by trifluoroacetic acid, which leads to the protonation of the aromatic carbon atoms followed by a cyclometallation at one *ortho* position. All the reactions involved in this process are represented in Scheme 2.

As we are measuring a reversible process which approaches to an equilibrium, the observed kinetic rate is a combination of the demetallation (k_1) and metallation (k_{-1}) processes, both depending on the acid concentration, equation (3).

$$A + H^+ \underset{}{\overset{K_a}{\rightleftharpoons}} HA^+ \underset{k_{-1}}{\overset{k_1}{\rightleftharpoons}} HB^+ \overset{K_b}{\rightleftharpoons} B + H^+ \quad (3)$$

Table 1 Measured values of k_{obs} of the *cis*-bridge substitution at different concentrations of CF_3CO_2H and CF_3CO_2D at 25 °C

$[CF_3CO_2H/D]/$ mol dm^{-3}	0.46	0.93	1.85	2.78	3.70	4.63	5.55
$10^4k_{obs(H)}/s^{-1}$	3.75	5.25	6.85	8.72	9.73	11.12	
$10^4k_{obs(D)}/s^{-1}$		4.30		7.50			10.30

Table 2 Values of k_{obs} for the *ortho*-phenyl D–H(H–D) exchange in **3D** at different concentrations of CF_3CO_2H at 45 °C

$[CF_3CO_2H]$/mol dm^{-3}	0.47	0.93	1.85	3.71	6.49	8.30
$10^6k_{obs}/s^{-1}$	17.1	22.5	30.1	46.4	56.6	67.3

Previous studies on electrophilic M–C bond cleavage[5] suggest that a tricentred transition state [M–C,H] is operating in these types of reactions. On that basis we assume that the HA^+ species in our scheme must contain a protonated trifluoroacetic acid in the axial co-ordination position adjacent to the Rh–C bond of the metallated phosphine. As for the HB^+ species the protonation of the equatorial trifluoroacetate group might be the most likely arrangement.

The rate equation (4) is derived from this scheme.

$$k_{obs} = (K_ak_1 + K_bk_{-1})[H^+]\,[H^+] \propto [CF_3CO_2H]^{\frac{1}{2}} \quad (4)$$

Under the experimental conditions used, the demetallated species is not detected, so we assume that $k_1 \ll k_{-1}$ and consequently $k_{obs} \approx K_bk_{-1}[H^+]$. A similar but much slower Rh–C activation was first observed for compound **1** in refluxing $MeCO_2D$. This is the first time that a study of the rate law has been made for this kind of reaction.

Crystal Structure of $[Rh_2(O_2CCF_3)_3\{(C_6H_4)PPh_2\}]\cdot 2CF_3CO_2H$ **3**.—A view of the molecular structure of compound **3** is shown in Fig. 2. Important bond distances and angles are given in Table 3. Fractional positional parameters are summarized in Table 4. In this structure the two rhodium atoms are bridged by three trifluoroacetate groups and one triphenylphosphine metallated in one phenyl ring; two oxygen atoms of two trifluoroacetic acid molecules occupying the axial positions complete the slightly distorted octahedral co-ordination around the metal centres [angles in the range 84.1(2)–97.0(2)°]. The Rh–Rh bond distance is 2.438(1) Å. The Rh–Rh–O axial angles are 172.1(1) and 168.9(2)°, slightly deviated from linearity. The Rh–O distances involving the axial trifluoroacetic acid are long and significantly different, 2.414(7) and 2.304(6) Å. Such differences must be attributed to the presence of the

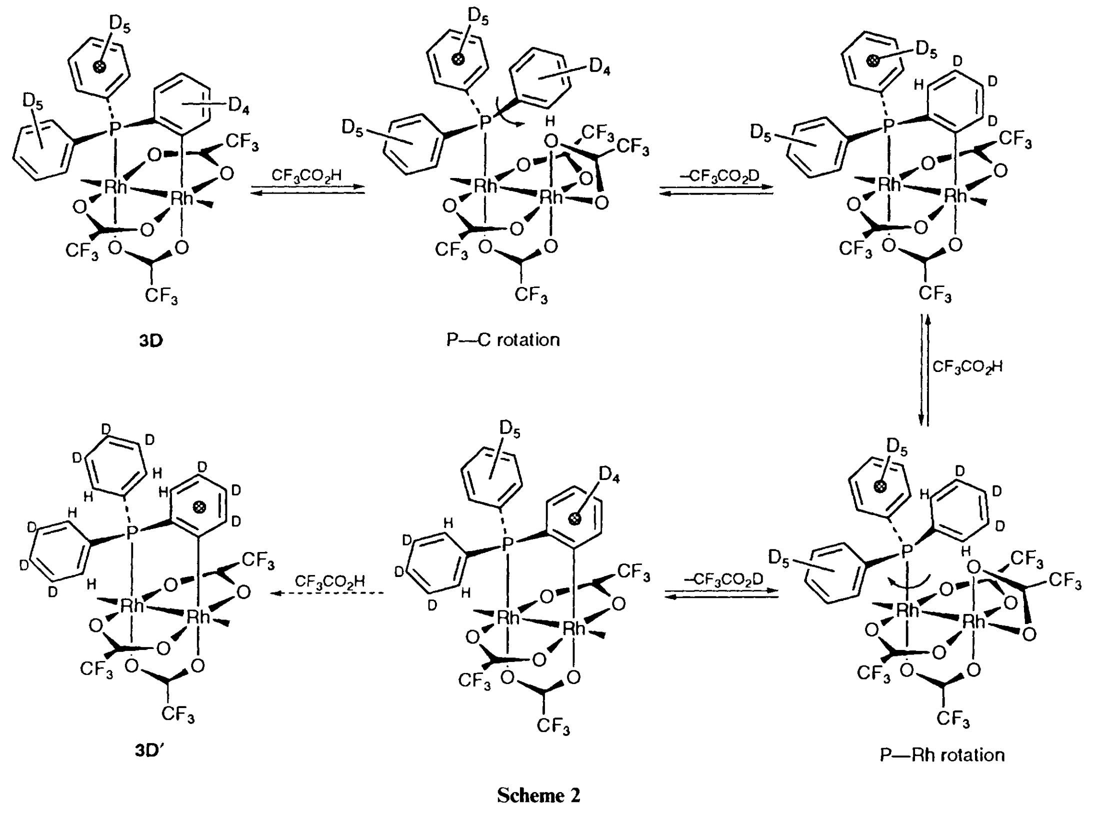

Scheme 2

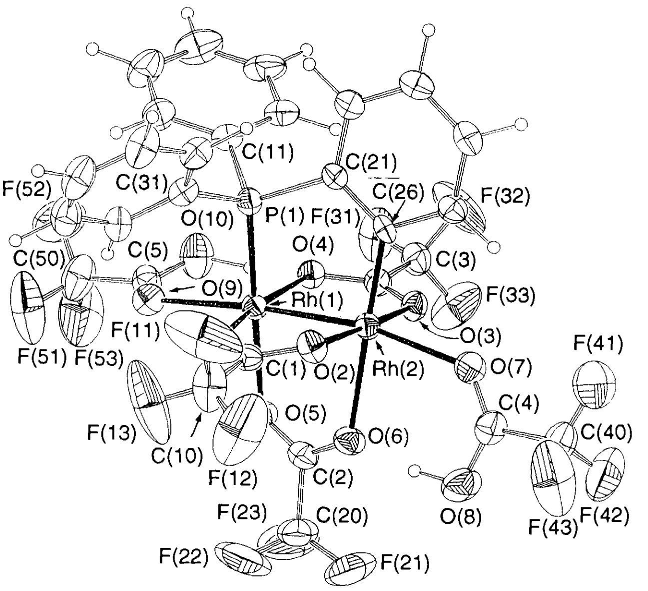

Fig. 2 Perspective view and atomic numbering of the compound **3**

Table 3 Selected bond lengths (Å) and angles (°) for compound **3** with estimated standard deviations (e.s.d.s) in parentheses

Rh(1)–Rh(2)	2.438(1)	O(3)–C(3)	1.23(1)
Rh(1)–O(4)	2.053(5)	O(6)–C(2)	1.25(1)
Rh(2)–O(2)	2.041(6)	O(9)–C(5)	1.14(1)
Rh(2)–O(7)	2.304(6)	C(2)–C(20)	1.52(1)
P(1)–C(21)	1.799(8)	C(5)–C(50)	1.51(2)
O(2)–C(1)	1.26(1)	Rh(1)–O(1)	2.043(6)
O(5)–C(2)	1.23(1)	Rh(1)–O(9)	2.414(7)
O(8)–C(4)	1.30(1)	Rh(2)–O(6)	2.240(6)
C(1)–C(10)	1.50(1)	P(1)–C(11)	1.805(9)
C(4)–C(40)	1.53(1)	O(1)–C(1)	1.25(1)
Rh(1)–P(1)	2.217(2)	O(4)–C(3)	1.276(9)
Rh(1)–O(5)	2.177(6)	O(7)–C(4)	1.19(1)
Rh(2)–O(3)	2.062(6)	O(10)–C(5)	1.33(1)
Rh(2)–C(26)	1.974(8)	C(3)–C(30)	1.51(1)
P(1)–C(31)	1.812(8)		
P(1)–Rh(1)–Rh(2)	90.5(1)	O(1)–Rh(1)–Rh(2)	86.2(2)
O(1)–Rh(1)–P(1)	91.9(2)	O(4)–Rh(1)–Rh(2)	87.4(1)
O(4)–Rh(1)–P(1)	92.3(2)	O(4)–Rh(1)–O(1)	172.4(2)
O(5)–Rh(1)–Rh(2)	88.6(2)	O(5)–Rh(1)–P(1)	179.2(2)
O(5)–Rh(1)–O(1)	88.3(2)	O(5)–Rh(1)–O(4)	87.4(2)
O(9)–Rh(1)–Rh(2)	172.1(2)	O(9)–Rh(1)–P(1)	96.5(2)
O(9)–Rh(1)–O(1)	97.0(2)	O(9)–Rh(1)–O(4)	88.8(2)
O(9)–Rh(1)–O(5)	84.3(2)	O(2)–Rh(2)–Rh(1)	87.6(2)
O(3)–Rh(2)–Rh(1)	87.0(2)	O(3)–Rh(2)–O(2)	174.5(2)
O(6)–Rh(2)–Rh(1)	84.1(2)	O(6)–Rh(2)–O(2)	86.9(2)
O(6)–Rh(2)–O(3)	91.7(2)	O(7)–Rh(2)–Rh(1)	168.9(2)
O(7)–Rh(2)–O(2)	91.3(2)	O(7)–Rh(2)–O(3)	93.9(2)
O(7)–Rh(2)–O(6)	84.8(2)	C(26)–Rh(2)–Rh(1)	96.5(2)
C(26)–Rh(2)–O(2)	93.5(3)	C(26)–Rh(2)–O(3)	88.0(3)
C(26)–Rh(2)–O(6)	179.3(3)	C(26)–Rh(2)–O(7)	94.6(3)

unsymmetrical metallated phosphine. Two monometallated dirhodium(II) compounds have been characterized as acetic acid adducts.[6,7] In one case,[7] a similar difference is found for the two axial Rh–O bond distances. In all these adducts the OH groups of the axial acetic acid molecules show intramolecular interaction with two oxygen atoms; in the previous monometallated compounds[6,7] the interaction is established with two oxygen atoms of the same bridging acetate, the one opposite to the metallated phosphine, through intramolecular hydrogen bonds. In the present case, H(101) is connected to O(6) by a strong hydrogen-bonding interaction [O(6) $\cdots$ O(8) 2.60(1) Å]. In contrast, the other axial acetic acid molecule does not show such an intramolecular interaction. This difference probably results in the different bond lengths of Rh(1)–O(9) and Rh(2)–O(7). The equatorial Rh–O distances are in the range 2.041(6)–2.240(6) Å, those *trans* to carbon or phosphorus atoms being longer than the rest in agreement with the *trans* effect of the Rh–C and Rh–P bonds. The torsion angles about the rhodium–rhodium bond are in the range 7.9(2)–12.6(2)°, indicating that the structure is closer to the eclipsed conformation than to the staggered one.

Experimental

General Comments.—The compounds $[Rh_2(O_2CMe)_3\{(C_6H_4)PPh_2\}]\cdot 2MeCO_2H$ **1** and $[Rh_2(O_2CMe)_3\{(C_6D_4)P(C_6D_5)_2\}]\cdot 2MeCO_2H$ **1D**, were prepared according to literature methods[6b] using PPh_3 and $P(C_6D_5)_3$ respectively. Commercially available $P(C_6D_5)_3$ (Aldrich), CF_3CO_2H and $CDCl_3$ were used as purchased. Proton NMR measurements were recorded in Bruker AC-200, Varian-300 and Varian-400 spectrometers. All solvents were of analytical grade. Chloroform and toluene were dried and degassed before use; acetic acid was only degassed.

Synthesis of Compounds.—$[Rh_2(O_2CMe)_{2cis}(O_2CCF_3)_{trans}\{(C_6H_4)PPh_2\}]\cdot 2CF_3CO_2H$ **4**. Compound **1** (100 mg, 0.13 mmol) was dissolved in $CHCl_3$ (2 cm^3) and CF_3CO_2H (0.25 cm^3) added to the deep violet solution which immediately turned green. Removal of the solvent under vacuum gave a crude green solid which was recrystallized from CH_2Cl_2–hexane (10 cm^3, 1:1) yielding $[Rh_2(O_2CMe)_{2cis}(O_2CCF_3)_{trans}\{(C_6H_4)PPh_2\}]\cdot 2CF_3CO_2H$ **4** (yield 80%). NMR: $^{31}P-\{^1H\}$, δ 16.11 ($^1J_{Rh-P}$ = 143.7, $^2J_{Rh-P}$ = 4.1 Hz); ^1H, δ 1.25 (6 H, s, CH_3), 6.3 (1 H, complex, aromatic) and 6.5–7.9 (14 H, m, aromatic) (Found: C, 36.30: H, 2.35. $C_{28}H_{22}F_9O_{10}PRh_2$ requires C, 36.70; H, 2.70%).

$[Rh_2(O_2CCF_3)_3\{(C_6H_4)PPh_2\}]\cdot 2CF_3CO_2H$ **3** *and* $[Rh_2(O_2CCF_3)_3\{(C_6D_4)P(C_6D_5)_2\}]\cdot 2CF_3CO_2H$ **3D**. Compound **1** (50 mg, 0.065 mmol) was dissolved in $CHCl_3$ (1 cm^3) and CF_3CO_2H (1 cm^3) added. The green solution was stirred at room temperature for 24 h. The crude green solid was recrystallized from CH_2Cl_2–hexane (1:1, 10 cm^3) yielding $[Rh_2(O_2CCF_3)_3\{(C_6H_4)PPh_2\}]\cdot 2CF_3CO_2H$ **3** (yield 82%). NMR: $^{31}P-\{^1H\}$, δ 14.37 ($^1J_{Rh-P}$ = 139.2, $^2J_{Rh-P}$ = 3.9 Hz); ^1H, δ 6.4 (1 H, complex, aromatic) and 6.7–8.1 (14 H, m, aromatic) (Found: C, 32.50; H, 1.55. $C_{28}H_{16}F_{15}O_{10}PRh_2$ requires C, 32.60; H, 2.00%). The preparation of the compound $[Rh_2(O_2CCF_3)_3\{(C_6D_4)P(C_6D_5)_2\}]\cdot 2CF_3CO_2H$ **3D** is similar to that above except that **1D** was used as the starting compound and CF_3CO_2D as the carboxylic acid.

$[Rh_2(O_2CCF_3)_{2cis}(O_2CMe)_{trans}\{(C_6H_4)PPh_2\}]\cdot 2MeCO_2H$ **5**. Compound **3** (100 mg, 0.10 mmol) was dissolved in $CHCl_3$ (1 cm^3) and $MeCO_2H$ was added to the green solution which immediately turned violet. Removal of the solvent under vacuum gave a crude solid which was recrystallized from CH_2Cl_2–hexane (10 cm^3, 1:1) yielding $[Rh_2(O_2CCF_3)_{2cis}(O_2CMe)_{trans}\{(C_6H_4)PPh_2\}]\cdot 2MeCO_2H$ **5** (yield 92%). NMR: $^{31}P-\{^1H\}$, δ 15.62 ($^1J_{Rh-P}$ = 140.1, $^2J_{Rh-P}$ = 5.4 Hz); ^1H, δ 2.14 (6 H, s, CH_3), 2.21 (3 H, s, CH_3), 6.3 (1 H, complex, aromatic) and 6.5–7.9 (14 H, m, aromatic).

Reaction of **2D′** *with* CF_3CO_2H. Compound **2D′** (50 mg, 0.048 mmol) was dissolved in $CDCl_3$–CF_3CO_2H (0.7 cm^3, 1:1). The solution immediately turned green. The ^{31}P and ^1H spectra were recorded from the freshly prepared solution (t < 5 min). NMR: $^{31}P-\{^1H\}$ δ 15.28 ($^1J_{Rh-P}$ = 160.1 Hz), ^1H, δ 2.21 (12 H, s, CH_3). The same sample was introduced in a thermostatted bath (50 °C) for 36 h. No change was observed in the aromatic region of the ^1H NMR spectrum.

Kinetic Measurements.—*Kinetics of the reaction of compound* **1** *with* CF_3CO_2H *and* CF_3CO_2D. Compound **1** (40 mg, 0.049 mmol) was added to an NMR tube and was dissolved in $CDCl_3$–CF_3CO_2H (0.7 cm^3). The probe of the NMR spectrometer was

Table 4 Fractional positional parameters for compound **3** with e.s.d.s in parentheses

Atom	*x*	*y*	*z*	Atom	*x*	*y*	*z*
Rh(1)	0.203 95(5)	0.167 04(3)	0.236 71(5)	C(16)	0.397 4(8)	0.025 1(4)	0.209 8(7)
Rh(2)	0.040 57(6)	0.133 32(3)	0.177 40(5)	C(21)	0.145 1(7)	0.019 3(4)	0.256 3(6)
P(1)	0.229 0(2)	0.072 9(1)	0.323 6(2)	C(22)	0.163 1(8)	−0.044 3(4)	0.263 3(7)
O(1)	0.104 7(5)	0.189 8(3)	0.380 0(4)	C(23)	0.100 9(8)	−0.085 2(5)	0.207 2(7)
O(2)	−0.038 5(5)	0.142 0(3)	0.310 5(4)	C(24)	0.023 0(8)	−0.060 7(5)	0.143 2(7)
O(3)	0.132 9(5)	0.128 6(3)	0.049 4(4)	C(25)	0.004 8(7)	0.002 5(4)	0.137 1(6)
O(4)	0.286 8(4)	0.147 2(3)	0.134 8(4)	C(26)	0.065 0(6)	0.044 1(4)	0.194 9(6)
O(5)	0.177 6(5)	0.258 9(3)	0.203 3(4)	C(31)	0.203 1(6)	0.066 9(4)	0.456 6(6)
O(6)	0.011 9(5)	0.234 3(3)	0.155 8(5)	C(32)	0.239 7(8)	0.114 4(5)	0.519 2(7)
O(7)	−0.120 5(5)	0.121 5(3)	0.092 8(5)	C(33)	0.221 4(9)	0.109 6(6)	0.622 3(8)
O(8)	−0.176 0(6)	0.218 7(4)	0.072 1(7)	C(34)	0.169.5(9)	0.060 3(7)	0.661 5(8)
O(9)	0.367 5(5)	0.211 2(3)	0.331 5(5)	C(35)	0.133 0(8)	0.015 5(6)	0.601 0(8)
O(10)	0.477 8(6)	0.187 9(4)	0.204 2(6)	C(36)	0.149 7(7)	0.018 1(5)	0.496 2(7)
C(1)	0.009 3(8)	0.171 2(4)	0.378 7(7)	F(11)	−0.075(1)	0.139 2(5)	0.520 2(9)
C(10)	−0.058(1)	0.187 1(9)	0.468 5(9)	F(12)	−0.148 7(9)	0.202 9(8)	0.452 9(7)
C(2)	0.087 3(8)	0.271 2(4)	0.171 2(7)	F(13)	−0.016 6(9)	0.219 5(7)	0.530 5(8)
C(20)	0.061(1)	0.338 4(6)	0.150(1)	F(21)	−0.018 0(7)	0.347 4(3)	0.094 0(8)
C(3)	0.231 8(8)	0.133 3(4)	0.057 1(6)	F(22)	0.052(1)	0.368 3(5)	0.228 9(8)
C(30)	0.297 1(9)	0.120 7(5)	−0.036 1(7)	F(23)	0.141 1(8)	0.365 7(4)	0.104(1)
C(4)	−0.183 4(8)	0.159 2(6)	0.065 2(7)	F(31)	0.400 5(6)	0.126 1(4)	−0.026 4(5)
C(40)	−0.290(1)	0.139 7(8)	0.015(1)	F(32)	0.282 4(7)	0.063 0(4)	−0.063 8(7)
C(5)	0.448(1)	0.213 2(5)	0.290 8(8)	F(33)	0.266 4(6)	0.152 9(5)	−0.111 2(5)
C(50)	0.549(1)	0.240 5(8)	0.337(1)	F(41)	−0.291 7(6)	0.081 8(5)	−0.003 4(8)
C(11)	0.366 7(7)	0.047 7(4)	0.305 7(7)	F(42)	−0.295 2(7)	0.162 7(5)	−0.075 1(7)
C(12)	0.445 6(7)	0.053 9(5)	0.379 2(8)	F(43)	−0.369 4(7)	0.156 6(7)	0.058 2(9)
C(13)	0.550 1(8)	0.037 2(6)	0.357 4(9)	F(51)	0.526 7(8)	0.270 5(6)	0.416 8(8)
C(14)	0.579 5(9)	0.016 9(6)	0.262(1)	F(52)	0.622 1(8)	0.204 8(5)	0.356(1)
C(15)	0.504(1)	0.010 4(5)	0.192 1(9)	F(53)	0.589 3(8)	0.282 9(5)	0.282 2(7)

Table 5 Crystallographic data for compound **3**

Crystal colour	Dark green
Crystal size (mm)	0.20 × 0.20 × 0.10
Formula	$C_{28}H_{16}F_{15}O_{10}PRh_2$
M	1032.17
Space group	$P2_1/n$
a/Å	12.369(2)
b/Å	21.711(6)
c/Å	13.367(2)
β/°	90.11(2)
U/Å^3	3590(1)
Z	4
λ/Å	0.710 73
D_c/g cm^{-3}	1.91
μ(Mo-Kα)/cm^{-1}	10.75
Drift corrections	0.98–1.00
F(000)	2008

equilibrated at 298, 303 or 308 K. The exchange of the *cis* bridges was monitored by recording ^{1}H NMR spectra of the sample every 5 min and measuring the decrease of the signal at δ 1.25 corresponding to the *cis* $MeCO_2^-$ groups. In the experiments run with concentrations of CF_3CO_2H lower than 1 mol dm^{-3}, two different rates were detected for the substitution of the two *cis* acetate bridges, but only the slower one could be measured. The total intensity of all the methyl resonances, $\Sigma I(CH_3)$, was taken as internal reference. This value corresponds to 5 methyl groups per mol of rhodium dimer. The percentage of protonated *cis* methyl groups is given by 100*R*, where $R = \frac{5}{2}[I(MeCO_2{}^-{}_{cis})/\Sigma I(CH_3)]$. A plot of ln *R vs.* time was linear with correlation coefficients within the range 0.992–0.999. Activation parameters for the exchange reaction were calculated from the corresponding Eyring plots according to the data obtained from variable-temperature measurements.

Kinetics of the D–H *exchange in* **3D**. Compound **3D** (25 mg, 0.025 mmol) was introduced in an NMR tube and dissolved in $CDCl_3$–CF_3CO_2H. The NMR probe was equilibrated at 45 °C. The Rh–C activation was monitored by measuring the increase of the two doublets in the aromatic region at δ 6.88 and 7.49 taking the signal due to the acid proton as internal reference. The same procedure was used to measure the isotopic effect when using CF_3CO_2D and **3D′**, a derivative of compound **3D** in which the aromatic *ortho* positions are totally protonated, and measuring the decrease of intensity of these signals.

Crystallography.—A well formed green crystal of compound **3** grown by slow diffusion of hexane into a solution of **3** in CH_2Cl_2–$MeCO_2H$ (1 : 1) was used for the structure determination. A Nonius CAD4 single-crystal diffractometer was used. Unit-cell dimensions were determined from the angular settings of 25 reflections with θ in the range 15–20°. The space group $P2_1/n$ was determined from systematic absences. 6743 Reflections were collected in the *hkl* range −14 to 14, 0–25, 0–15 with $0 < \theta < 25°$ and 3570 independent reflections with $I > 3\sigma(I)$ were used for the analysis. The ω–2θ scan technique was used with a variable scan rate and a maximum scan time of 60 s per reflection. The structure was solved by Patterson interpretation, using the program SHELX 86[8] and expanded with DIRDIF.[9] Isotropic least-squares refinement was performed using a locally modified version of the SHELX 76 program.[10] At this stage an additional empirical absorption correction was applied.[11] The final conventional agreement factors were $R = 0.044$ and R' $[=\Sigma w(F_o - F_c)^{\frac{1}{2}}$ where $w^{-1} = \sigma^2(F_o) + 0.0003F_o{}^2] = 0.044$ for the 3570 observed reflections and 506 variables. Geometrical calculations were made with PARST,[12] and the molecule drawn with the PLUTO program.[13] Calculations were performed on a VAX 4000 at the Departamento de Química Física of the University of Valencia.

Crystallographic parameters and remaining experimental details for the structure are collected in Table 5.

Additional material available from the Cambridge Crystallographic Data Centre comprises H-atom coordinates, thermal parameters and remaining bond lengths and angles.

Electrochemical Measurements.—The electrochemical experiments were carried out in a three-electrode cell; the working and auxiliary electrodes were platinum and the reference electrode was a saturated calomel electrode electrically connected to the solution by a salt bridge containing a saturated solution of the supporting electrolyte and the solvent. Cyclic voltammograms were obtained with a programming function generator 305 HQ instrument connected to a AMEL potentiostat, and were recorded on a RIKEN-DENSHI F-35 *x–y* recorder. The solvent was CH_2Cl_2 which had been freshly distilled from P_2O_5. The supporting electrolyte, NBu_4PF_6, was recrystallized from ethanol and dried at 80 °C under vacuum for 48 h.

Cyclic voltammetry of compound **3** was performed to enable a comparison of its electrochemical behaviour with that of other related metallated products such as $[Rh_2(O_2CMe)_3\{(C_6H_4)PPh_2\}]\cdot 2MeCO_2H$ **1**, which has been described previously.[14]

Compound **3** exhibits by cyclic voltammetry a partially reversible oxidation peak at $E_{\frac{1}{2}}$ 1.55 V. This value is clearly higher than that observed for the acetate-bridged derivative **1** (1.02 V)[14] and reflects the strong effect of the electron-demanding character of the trifluoroacetate bridges on the dinuclear unit.

Acknowledgements

We thank the Comisión Interministerial de Ciencia y Tecnologia for financial support and Dr. Wladimiro Díaz for computing assistance. We appreciate the comments of Professor Martinho Simoes during this work.

References

1 P. Lahuerta and E. Peris, *Inorg. Chem.*, 1992, **31**, 4547.
2 E. C. Morrison and D. A. Tocher, *Inorg. Chim. Acta*, 1989, **156**, 99.
3 J. Kitchens and J. L. Bear, *J. Inorg. Nucl. Chem.*, 1969, **31**, 2415.
4 R. A. Walton and F. A. Cotton, *Multiple Bonds between Metal Atoms*, Clarendon Press, Oxford, 1993, ch. 7; T. R. Felthouse, *Prog. Inorg. Chem.*, 1982, **29**, 74.
5 U. Belluco and B. Crociani, *J. Organomet. Chem.*, 1983, **250**, 565; P. Lahuerta, E. Peris, M. A. Ubeda, S. García Granda, F. Gómez Beltrán and M. R. Díaz, *J. Organomet. Chem.*, 1993, **455**, C10.
6 (*a*) P. Lahuerta, J. Payá, E. Peris, M. A. Pellinghelli and A. Tiripicchio, *J. Organomet. Chem.*, 1989, **373**, C5; (*b*) P. Lahuerta, J. Payá, M. A. Pellinghelli and A. Tiripicchio, *Inorg. Chem.*, 1992, **31**, 1224 and refs. therein.
7 P. Lahuerta, J. Payá, X. Solans and M. A. Ubeda, *Inorg. Chem.*, 1992, **32**, 385.
8 G. M. Sheldrick, C. Kruger and R. Goddard, *Crystallographic Computing*, Clarendon Press, Oxford, 1985, p. 175.
9 P. T. Beurskens, G. A. G. Beurskens, W. P. Bosman, S. García-Granda, R. O. Gould, J. M. M. Smits and C. Smykalla, The DIRDIF program system, Technical Report of the Crystallography Laboratory, University of Nijmegen, 1992.
10 G. M. Sheldrick, SHELX 76, program for crystal structure determination, University of Cambridge, 1976.
11 N. Walker and D. Stuart, *Acta Crystallogr., Sect. A*, 1983, **39**, 158.
12 M. Nardelli, *Comput. Chem.*, 1983, **7**, 95.
13 A. L. Spek, The EUCLID package, in *Computational Crystallography*, ed. D. Sayre, Clarendon Press, Oxford, 1982, p. 528.
14 F. Estevan, P. Lahuerta, J. Latorre, E. Peris, S. García-Granda, F. Gómez-Beltrán, A. Aguirre and M. A. Salvadó, *J. Chem. Soc., Dalton Trans.*, 1993, 1681; F. Estevan, J. Latorre and E. Peris, *Polyhedron*, 1993, **12**, 2153.

Received 15*th June* 1993; *Paper* 3/03454B